marine drugs

Article

Chemical Diversity from a Chinese Marine Red Alga, *Symphyocladia latiuscula*

Xiuli Xu [1], Haijin Yang [1,2], Zeinab G. Khalil [3], Liyuan Yin [1], Xue Xiao [3], Pratik Neupane [3], Paul V. Bernhardt [4], Angela A. Salim [3], Fuhang Song [2,*] and Robert J. Capon [3,*]

1 School of Ocean Sciences, China University of Geosciences, Beijing 100083, China; xuxl@cugb.edu.cn (X.X.); yanghaijin52@163.com (H.Y.); yinliyuan999@sina.com (L.Y.)
2 CAS Key Laboratory of Pathogenic Microbiology and Immunology, Institute of Microbiology, Chinese Academy of Sciences, Beijing 100101, China
3 Institute for Molecular Bioscience, The University of Queensland, Brisbane, QLD 4072, Australia; z.khalil@uq.edu.au (Z.G.K.); x.xue@uq.edu.au (X.X.); p.neupane@imb.uq.edu.au (P.N.); a.salim@uq.edu.au (A.A.S.)
4 School of Chemistry and Molecular Biosciences, The University of Queensland, Brisbane, QLD 4072, Australia; p.bernhardt@uq.edu.au
* Correspondence: songfuhang@im.ac.cn (F.S.); r.capon@uq.edu.au (R.J.C.); Tel.: +86-10-6480-6058 (F.S.); +61-7-3346-2979 (R.J.C.)

Received: 3 November 2017; Accepted: 23 November 2017; Published: 1 December 2017

Abstract: This study describes an investigation into secondary metabolites that are produced by a marine red alga, *Symphyocladia latiuscula*, which was collected from coastal waters off Qingdao, China. A combination of normal, reversed phase, and gel chromatography was used to isolate six citric acid derived natural products, aconitates A–F (**1**–**6**), together with two known and ten new polybrominated phenols, symphyocladins C/D (**7a/b**), and symphyocladins H–Q (**8a/b**, **9a/b** and **10**–**15**), respectively. Structure elucidation was achieved by detailed spectroscopic (including X-ray crystallographic) analysis. We propose a plausible and convergent biosynthetic pathway involving a key quinone methide intermediate, linking aconitates and symphyocladins.

Keywords: marine red alga; *Symphyocladia latiuscula*; bromophenols; symphyocladins; aconitates

1. Introduction

Historically, natural products have inspired the development of many pharmaceuticals and agrochemicals, which, have in turn, played an important role in improving human and animal health and agricultural productivity, enhancing the quality of life for communities across the globe [1]. One of the defining characteristics of natural products is their structure diversity, which can encompass complex carbocyclic and heterocyclic scaffolds, annotated with a wide array of functional groups and stereochemical features. As such, even a limited set of biosynthetic precursors can deliver remarkable chemical diversity. Illustrative of this phenomenon are bromophenols from marine red algae (Rhodophyta) [2–20]. For example, the red alga *Symphyocladia latiuscula* (Harvey) Yamada has been reported to produce a diverse array of bromophenols elaborated by sulfoxides, sulphones, sulfates, glutamines, pyrrolidin-2-ones, ureas, diketopiperazines, and aconitic acids, with biological properties spanning antibacterial [11,12], antifungal [10–14], antiviral [15], anticancer [16], free radical scavenging [9,17,18], aldose reductase inhibitory [19], and Taq DNA polymerase inhibitory activities [20]. *S. latiuscula* bromophenols typically contain at least one 2,3,6-tribromo-4,5-dihydroxybenzyl moiety, as consistent with a highly conserved biosynthetic pathway. This report described our efforts to further elaborate the chemical diversity of *S. latiuscula*.

2. Results and Discussion

The EtOAc extract of a Chinese collection of *S. latiuscula* was concentrated *in vacuo* and subjected to a sequence of normal, reversed phase, and gel chromatography, with HPLC-MS analysis being used to prioritize fractions of interest. Following this strategy, we isolated and characterized six citric acid derived natural products, aconitates A–F (**1–6**), together with two known and ten new polybrominated phenol adducts, symphyocladins C/D (**7a/b**), and symphyocladins H–Q (**8a/b**, **9a/b** and **10–15**), respectively (Figure 1). A spectroscopic analysis approach (see Tables 1–5) to the structure elucidation of all of these metabolites is summarized below.

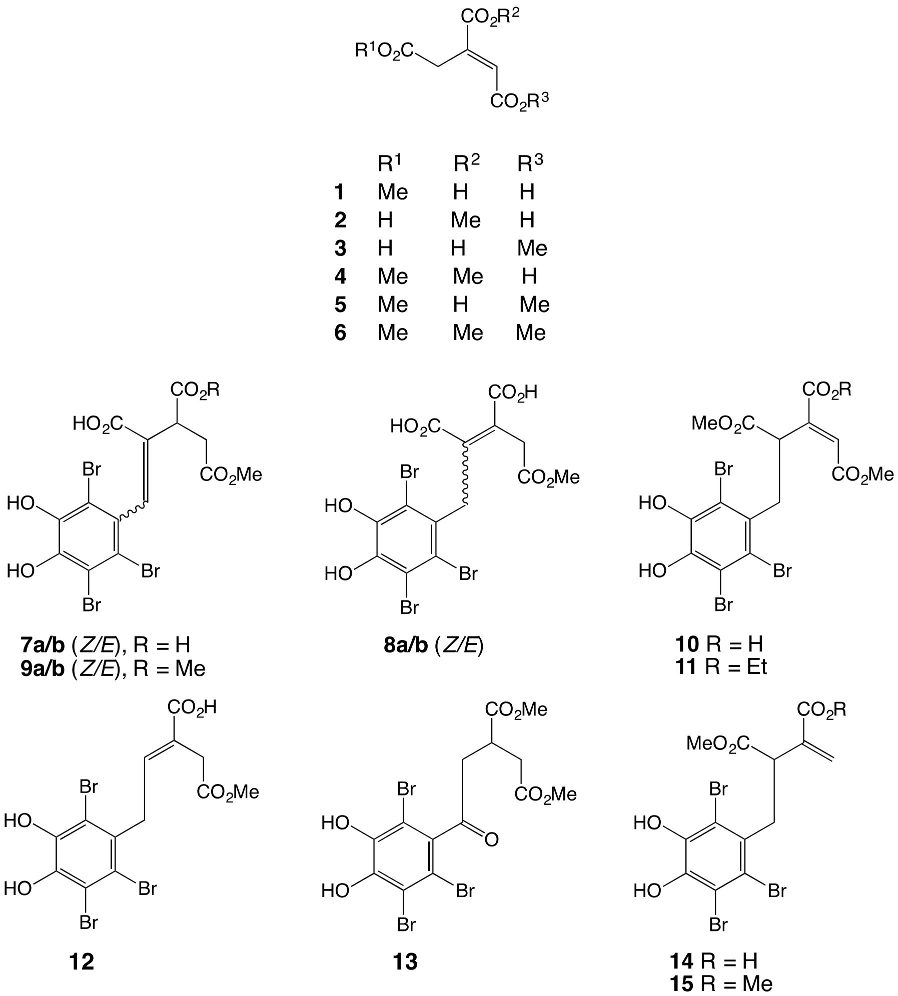

Figure 1. *S. latiuscula* metabolites **1–15**.

HRESI(+)MS measurements confirmed that **1** ($C_7H_8O_6$, Δmmu +0.2), **2** ($C_7H_8O_6$, Δmmu +0.1) and **3** ($C_7H_8O_6$, Δmmu +0.1) were isomeric, while analysis of the one-dimensional (1D) and two-dimensional (2D) NMR (methanol-d_4) data (Figures S8–S13, Tables S2 and S3) suggested they were mono methyl esters of *E*-aconitic acid, for which we attribute the trivial names aconitates A–C. Assignment of *E* $\Delta^{3,4}$ configurations were inferred from diagnostic chemical shifts for H-4 and C-2 in **1** (δ_H 6.92; δ_C 33.8), **2** (δ_H 6.89; δ_C 33.9), and **3** (δ_H 6.91; δ_C 33.9), when compared to the authentic standards for *E* (δ_H 6.90; δ_C 33.8) and *Z* (δ_H 6.26; δ_C 40.2) aconitic acid (Figures S1–S7, Table S1). HMBC correlations permitted assignment of the methyl ester regiochemistry across **1–3** with correlations from (i) the OMe (δ_H 3.67) and H_2-2 (δ_H 3.89) to C-1 (δ_C 172.7) confirming a C-1 CO_2Me in aconitate A (**1**), (ii) the OMe (δ_H 3.81) and H_2-2 (δ_H 3.89) to C-6 (δ_C 168.4) confirming a C-6 CO_2Me in aconitate B (**2**), and (iii) the OMe (δ_H 3.77) and H-4 (δ_H 6.91) to C-5 (δ_C 167.5) confirming a C-5 CO_2Me in aconitate C (**3**) (Figure 2).

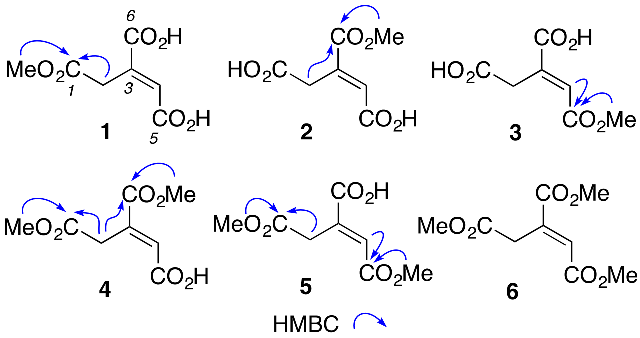

Figure 2. Diagnostic 2D NMR (methanol-d_4) correlations for aconitates A–F (**1**–**6**).

HRESI(+)MS measurements suggested that **4** ($C_8H_{10}O_6$, Δmmu +0.2) and **5** ($C_8H_{10}O_6$, Δmmu +0.2) were isomeric dimethyl esters, and **6** ($C_9H_{12}O_6$, Δmmu +0.1) was a trimethyl ester, of aconitic acid. Analysis of the NMR (methanol-d_4) data for **4**–**6** (Figures S14–S19, Tables S3 and S4) confirmed these assignments, with *E* $\Delta^{3,4}$ configurations being inferred from diagnostic chemical shifts for H-4 and C-2 in aconitate D (**4**) (δ_H 6.91; δ_C 33.8), aconitate E (**5**) (δ_H 6.92; δ_C 33.9) and aconitate F (**6**) (δ_H 6.92; δ_C 33.8), and HMBC correlations permitting the assignment of the dimethyl ester regiochemistry across **4** and **5**. For example, correlations from an OMe (δ_H 3.67) and H_2-2 (δ_H 3.91) to C-1 (δ_C 172.5), and from an OMe (δ_H 3.80) and H_2-2 to C-6 (δ_C 168.2), confirmed the presence of C-1 CO_2Me and C-6 CO_2Me moieties in **4**, whereas correlations from an OMe (δ_H 3.67) and H_2-2 (δ_H 3.91) to C-1 (δ_C 172.5), and from an OMe (δ_H 3.76) and H-4 (δ_H 6.92) to C-5 (δ_C 167.5), confirmed C-1 CO_2Me and C-5 CO_2Me moieties in **5** (Figure 2).

HRESI(+)MS measurements confirmed that **7a/b** ($C_{14}H_{11}Br_3O_8$, Δmmu +0.5) and **8a/b** ($C_{14}H_{11}Br_3O_8$, Δmmu +0.4) were isomeric, and suggested that **9a/b** ($C_{15}H_{13}Br_3O_8$, Δmmu +0.4) and **10** ($C_{15}H_{13}Br_3O_8$, Δmmu +0.5) were CH_2 homologues, and **11** ($C_{17}H_{17}Br_3O_8$, Δmmu +0.6) was a CH_2CH_2 homologue of **7a/b** and **8a/b**. Analysis of the NMR (acetone-d_6) data for **7a/b** (Figures S20 and S21, Table 1, Table 2 and Table S5) confirmed them as symphyocladins C/D, first reported in 2012 from *S. latiuscula* as an inseparable mixture of *Z*/*E* $\Delta^{2,7'}$ isomers [13]. Analysis of the NMR (methanol-d_4) data for symphyocladins H/I (**8a/b**) (Figures S22–S27, Table 1, Table 2 and Table S6) revealed $\Delta^{2,3}$ and C-5 CO_2Me moieties, as evidenced by diagnostic HMBC correlations (Figure 3). Significantly, these data also revealed an interconverting mixture of *E*/*Z* $\Delta^{2,3}$ isomers, in which the minor *Z* isomer, symphyocladin H (**8a**), as evidenced by a ROESY correlation between H_2-4 and H_2-7′ (Figure 3), was in equilibrium with the major *E* isomer, symphyocladin I (**8b**). Further analysis of this NMR data revealed chemical shift differences diagnostic for $\Delta^{2,3}$ geometric isomers; H_2-4 (*E* δ_H 3.65, δ_C 35.0; *Z* δ_H 3.19, δ_C 29.5), C-1 (*E* δ_C 170.3; *Z* δ_C 166.5), C-3 (*E* δ_C 127.4; *Z* δ_C 137.8), and C-5 CO_2Me (*E* δ_H 3.71; *Z* δ_H 3.51). Remarkably, the NMR (acetonitrile-d_3) data for **8a/b** revealed a single *Z* isomer **8a**, as evidenced by simplified spectra, a ROESY correlation between H_2-4 and H_2-7′, and diagnostic chemical shifts (Figures S28 and S29, Table S7). We speculate that in aprotic solvents (i.e., acetonitrile-d_3), hydrogen bonding between adjacent CO_2H moieties exclusively favors the lower energy *Z* $\Delta^{2,3}$ isomer. By contrast, in protic solvents (i.e., methanol-d_4), the disruption of this hydrogen bonding favor equilibration to an *E*/*Z* $\Delta^{2,3}$ mixture dominated by the less sterically constrained *E* isomer. This observation highlights the critical importance that NMR solvents can play in the analysis and structure elucidation of natural products.

Analysis of the NMR (DMSO-d_6) data for symphyocladins J/K (**9a/b**) (Figures S30 and S31, Table 1, Table 2 and Table S8) identified an inseparable mixture of C-6 CO_2Me homologues of **7a/b** and **8a/b**, as evidenced by spectroscopic comparisons and diagnostic HMBC correlations from the additional

$CO_2\underline{Me}$ resonances to C-6 (Figure 3). In this instance, as hydrogen bonding does not stabilize double bond isomers, the *Z*/*E* mixture prevails even in an aprotic solvent (i.e., DMSO-d_6). Analysis of the NMR (acetone-d_6) data for symphyocladin L (**10**) (Figures S32 and S33, Table 3, Table 5 and Table S9) revealed a $\Delta^{3,4}$ isomer and 1-CO_2Me homologue of **7a/b** and **8a/b**, as evidenced by COSY correlations between H-2 and H_2-7′, and diagnostic HMBC correlations positioning both C-1 CO_2Me and C-5 CO_2Me (Figure 3). The structure of **10** inclusive of an *E* $\Delta^{3,4}$ configuration and its racemic nature were confirmed by single crystal X-ray analysis with the compound crystallizing in a centrosymmetric space group (Figures S34 and S35). Analysis of the NMR (methanol-d_4) data for symphyocladin M (**11**) (Figures S36 and S37, Table 3, Table 5 and Table S10) revealed it as a C-6 CO_2Et homologue of **10**, as evidenced by spectroscopic comparisons and an HMBC correlation from the $CO_2\underline{Et}$ moiety to C-6.

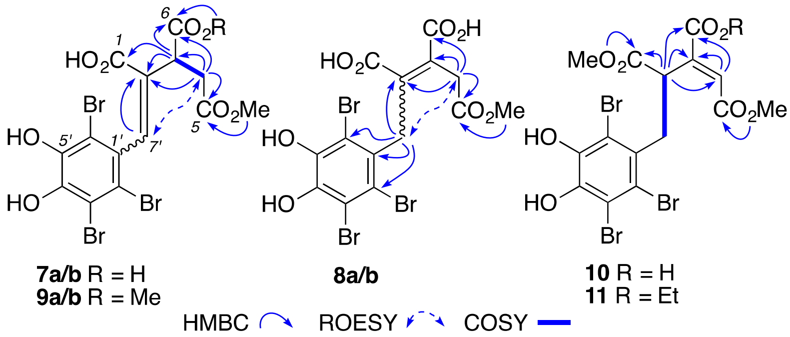

Figure 3. Diagnostic 2D NMR correlations for symphyocladins C/D (**7a/b**), H/I (**8a/b**), J/K (**9a/b**) and L–M (**10**–**11**) (see Tables and Supporting Information for NMR solvents).

Table 1. ^{1}H NMR Data for Compounds **7a/b**–**9a/b** (600 MHz).

Position	7a [a]	7b [a]	8a [b]	8b [b]	9a [c]	9b [c]
3	3.74, m	3.74, m			3.50, m	3.50, m
4a	3.17, m	3.17, m	3.65, s	3.19, s	2.98, dd [e]	2.976, dd [e]
4b	2.490, dd [d]	2.489, dd [d]			2.41, dd [f]	2.40, dd [f]
5-OCH3	3.55, s	3.55, s	3.71, s	3.51, s	3.52, s	3.52, s
6-OCH3					3.541, s	3.535, s
7′	7.544, s	7.538, s	4.22, s	4.34, s	7.391, s	7.388, s

[a] acetone-d_6, [b] methanol-d_4, [c] DMSO-d_6, [d] J = 16.8, 7.8 Hz, [e] J = 16.8, 10.8 Hz, [f] J = 16.8, 3.0 Hz.

Table 2. ^{13}C NMR Data for Compounds **7a/b**–**9a/b** (150 MHz).

Position	7a [a]	7b [a]	8a [b]	8b [b]	9a [c]	9b [c]
1	167.18, C	167.18, C	170.3, C	166.5, C	166.8, C	166.8, C
2	135.46, C	135.34, C	145.0, C	144.4, C	133.5, C	133.5, C
3	41.39, CH	41.37, CH	127.4, C	137.8, C	40.2, CH	40.2, CH
4	35.40, CH_2	35.35, CH_2	35.0, CH_2	29.5, CH_2	33.9, CH_2	33.9, CH_2
5	172.80, C	172.76, C	168.7, C	166.8, C	171.5, C	171.5, C
6	172.54, C	172.49, C	172.4, C	169.0, C	171.5, C	171.5, C
5-OCH_3	51.87, CH_3	51.83, CH_3	52.8, CH_3	53.1, CH_3	52.0, CH_3	52.0, CH_3
6-OCH_3					51.6, CH_3	51.6, CH_3
1′	129.79, C	129.76, C	128.8, C	127.9, C	128.07, C	128.07, C
2′	115.38, C	115.23, C	118.9, C	118.4, C	113.9, C	113.9, C
3′	113.98, C	113.63, C	114.8, C	114.2, C	113.7, C	113.6, C
4′	144.17, C	144.10, C	146.2, C	145.5, C	143.9, C	143.8, C
5′	145.36, C	145.32, C	145.6, C	144.8, C	145.2, C	145.0, C
6′	110.71, C	110.67, C	114.7, C	114.3, C	110.7, C	110.6, C
7′	141.52, C	141.48, C	41.1, CH	35.9, CH	140.7, C	140.7, C

[a] acetone-d_6, [b] methanol-d_4, [c] DMSO-d_6.

Table 3. ^{1}H NMR Data for Compounds **10–11** (600 MHz).

Position	10 [a] δ_H, m (J in Hz)	11 [b] δ_H, m (J in Hz)
2	4.98, dd (11.4, 3.0)	4.98, dd (11.4, 3.0)
4	6.76, s	6.73, s
1-OCH_3	3.66, s	3.70, s
5-OCH_3	3.44, s	3.45, s
6-$OC\underline{H}_2CH_3$		4.26, br q (7.2)
6-$OCH_2C\underline{H}_3$		1.31, t (7.2)
7′a	3.87, dd (14.4, 3.0)	3.81, dd (14.4, 3.0)
7′b	3.61, dd (14.4, 11.4)	3.56, dd (14.4, 11.4)

[a] acetone-d_6, [b] methanol-d_4.

Table 4. ^{1}H NMR Data for Compounds **12–15** (600 MHz).

Position	12 [a] δ_H, m (*J* in Hz)	13 [b] δ_H, m (*J* in Hz)	14 [b] δ_H, m (*J* in Hz)	15 [a] δ_H, m (*J* in Hz)
2a	6.79, br t (6.6)	3.35, m	3.75, dd (9.0, 6.0)	3.79, dd (9.6, 5.4)
2b		3.27, dd (20.4, 7.8)		
3		3.34, m		
4a	3.60, br s	2.86, dd (17.4, 7.2)	6.22. d (1.2)	6.17, d (1.2)
4b		2.73, dd (17.4, 6.0)	5.44, br s	5.52, s
1-OCH_3			3.64, s	3.62, s
5-OCH_3	3.66, s	3.68, s		
6-OCH_3		3.71, s		3.71, s
7′a	4.05, s		3.65, dd (13.8, 6.0)	3.69, dd (14.4, 5.4)
7′b			3.54, dd (13.8, 9.0)	3.56, dd (14.4, 9.6)

[a] acetone-d_6, [b] methanol-d_4.

Table 5. ^{13}C NMR Data for Compounds **10–15** (150 MHz).

Position	10 [a] δ_C, Type	11 [b] δ_C, Type	12 [a] δ_C, Type	13 [b] δ_C, Type	14 [b] δ_C, Type	15 [a] δ_C, Type
1	171.9, C	173.5, C			174.5, C	172.4, C
2	43.0, C	43.7, C	141.3, C	44.9, CH_2	48.8, CH	48.2, CH
3	142.4, C	142.4, C	128.1, C	37.4, CH	139.3, C	138.3, C
4	130.5, CH	131.3, CH	33.2, CH_2	35.6, CH_2	129.1, CH_2	128.7, CH_2
5	165.8, C	166.7, C	171.3, C	173.9, C		
6	167.0, C	167.0, C	167.9, C	175.5, C	169.2, C	166.6, C
1-OCH_3	52.3, CH_3	52.9, CH_3			52.8, CH_3	52.3, CH_3
5-OCH_3	52.1, CH_3	52.5, CH_3	52.0, CH_3	52.5, CH_3		
6-OCH_3				52.8, CH_3		52.3, CH_3
6-$O\underline{C}H_2CH_3$		63.2, C				
6-$OCH_2\underline{C}H_3$		14.5, CH_3				
1′	130.7, C	130.6, C	131.0, C	136.1, C	131.4, C	131.3, C
2′	118.5, C	118.8, C	117.3, C	114.5, C	118.3, C	118.0, C
3′	113.7, C	114.4, C	114.0, C	110.5, C	114.5, C	113.9, C
4′	144.1, C	145.1, C	144.4, C	147.3, C	145.0, C	144.0, C
5′	143.8, C	144.8, C	144.3, C	145.3, C	144.8, C	143.9, C
6′	114.3, C	114.8, C	113.0, C	106.3, C	114.3, C	113.8, C
7′	39.0, CH_2	39.4, CH_2	39.0, CH_2	202.2, C	39.4, CH_2	39.1, CH_2

[a] acetone-d_6, [b] methanol-d_4.

HRESI(+)MS measurements suggested that **12** ($C_{13}H_{11}Br_3O_6$, Δmmu +0.5) was a decarboxy analogue of **7a/b** and **8a/b**; **13** ($C_{14}H_{13}Br_3O_7$, Δmmu +0.5) was a dihydro oxidized methyl ester of **12**; **14** ($C_{13}H_{11}Br_3O_6$, Δmmu +0.5) was a decarboxymethyl analogue of **10**; and, **15** ($C_{14}H_{13}Br_3O_6$, Δmmu +0.5) was a CH_2 homologue of **14**. Comparison of the NMR (methanol-d_4) data for symphyocladin N (**12**) (Figures S38 and S39, Table 4, Table 5 and Table S11) with that for **8a/b** revealed the key difference as replacement of the C-1 CO_2H moiety in **8a/b** with an H-2 olefinic methine (δ_H 6.79) coupled to H_2-7′ (δ_H 4.05). The presence of a C-5 CO_2Me moiety in **12** was evident from an HMBC correlation from the OMe (δ_H 3.66) to C-5 (δ_C 171.3), while an *E* $\Delta^{2,3}$ configuration was confirmed by a ROESY correlation between H_2-4 (δ_H 3.60) and H_2-7′ (Figure 4). Analysis of the NMR (methanol-d_4)

data for symphyocladin O (**13**) (Figures S40 and S41, Table 4, Table 5, and Table S12) revealed it to be a saturated oxidized analogue of **12**, as evidenced by COSY correlations between a diastereotopic H_2-2 (δ_H 3.35/3.27), through H-3 (δ_H 3.34) to a diastereotopic H_2-4 (δ_H 2.86/2.73). Likewise, replacement of the C-7′ sp^3 methylene in **12** (δ_C 39.0) with a carbonyl resonance in 13 (δ_C 202.2) was evidence of a 7-oxo moiety. Diagnostic HMBC correlations also established the presence of incorporated C-5 $CO_2\underline{Me}$ (δ_H 3.68) and C-6 $CO_2\underline{Me}$ (δ_H 3.71) moieties (see Figure 3).

Comparison of the NMR (methanol-d_4) data for symphyocladin P (**14**) (Figures S42 and S43, Table 4, Table 5 and Table S13) with that for **10** revealed the key difference as replacement of the C-5 CO_2Me moiety in **10** with a diastereotopic H_2-4 olefinic methylene (δ_H 6.22/5.44). Comparison of the NMR (acetone-d_6) data for symphyocladin Q (**15**) (Figures S44 and S45, Table 4, Table 5 and Table S14) with that for **14** revealed the key difference as an additional resonance, attributed to a C-6 $CO_2\underline{Me}$ moiety (δ_H 3.71). Structure assignments for **14** and **15** were further supported by diagnostic 2D NMR correlations (Figure 4).

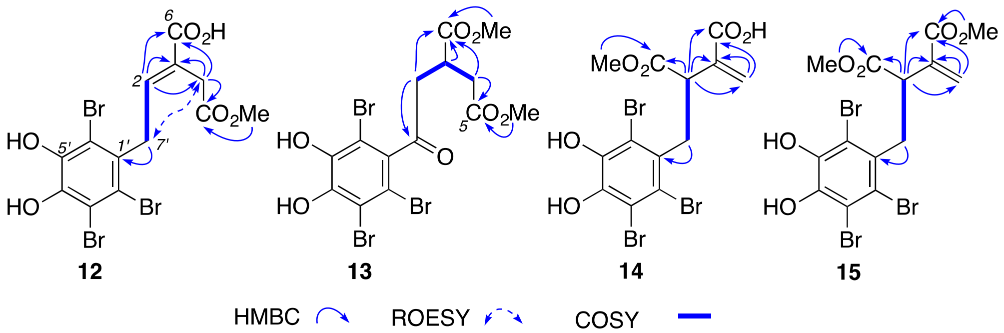

Figure 4. Diagnostic 2D NMR correlations for symphyocladins N–Q (**12**–**15**) (see Tables 4 and 5 and Supporting Information for NMR solvents).

Structural similarities across **1**–**15** suggest a highly conserved biosynthesis. Building on this observation, we propose a biosynthetic relationship (Figure 5), in which the aconitates A–F (**1**–**6**) are viewed as mono, di, and tri methyl esters of the precursor *E*-aconitic acid, itself a dehydration product of citric acid. Likewise, metabolites **7**–**15** can be viewed as adducts between aconitates and an intermediate quinone methide that is generated from 2,3,6-tribromo-4,5-dihydroxybenzyl alcohol, further elaborated by a combination of 1,3-hydride shifts, decarboxylations and oxidations. Although **7a/b**, **9a/b**, **10**–**11,** and **13** incorporate a single chiral sp^3 center, as they do not exhibit measurable optical rotations they are presumed to be racemic, as confirmed for **10** by X-ray crystallography. The absence of double bond migrations (i.e., racemization) during isolation and handling suggests that this racemic character is a function of achiral adduct addition. The proposed biosynthetic relationship informs a possible biomimetic synthesis of **7**–**15**, although, in our hands, synthetic 2,3,6-tribromo-4,5-dihydroxybenzyl alcohol proved stable to both acid and base conditions indicative of a requirement to activate the benzyl alcohol moiety to effect dehydration and the formation of a quinone methide.

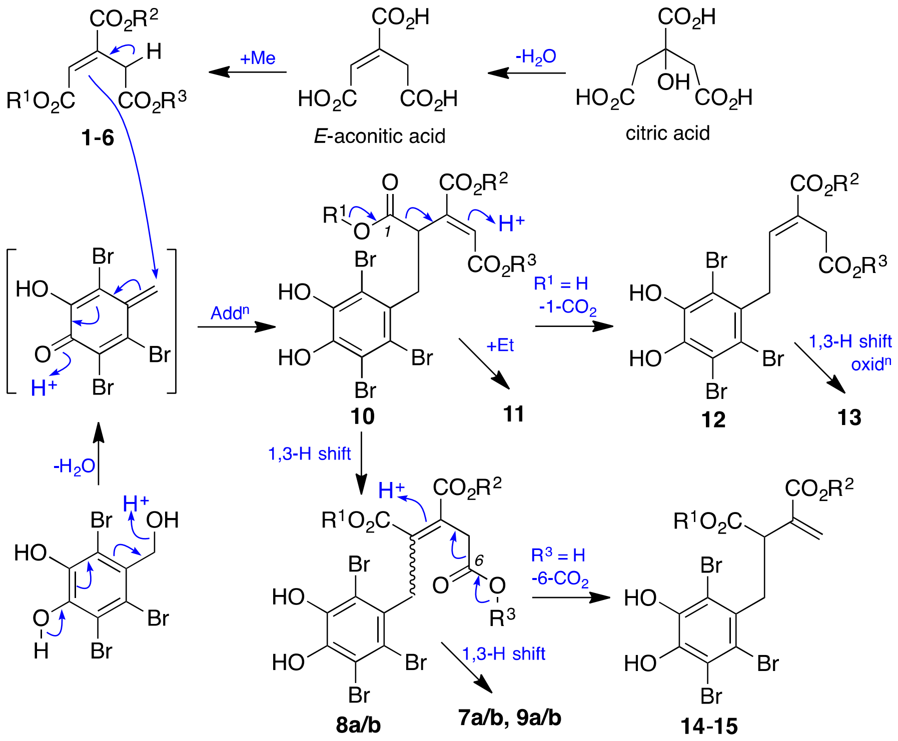

Figure 5. A plausible biosynthetic relationship linking **1–15**.

3. Materials and Methods

General Experimental Procedures. Specific optical rotations ($[\alpha]_D$) were measured on a polarimeter in a 100 × 2 mm cell at 22 °C. NMR spectra were obtained on a Bruker Avance DRX600 or DRX500 spectrometers, in the solvents indicated and referenced to residual ^1H and ^{13}C signals in deuterated solvents. Electrospray ionization mass spectra (ESIMS) were acquired using an Agilent 1100 Series separations module equipped with an Agilent 1100 Series LC/MSD mass detector in both positive and negative ion modes. High-resolution ESIMS measurements were obtained on a Bruker micrOTOF mass spectrometer by direct infusion in MeCN at 3 mL/min using sodium formate clusters as an internal calibrant. HPLC was performed using an Agilent 1100 Series separations module equipped with Agilent 1100 Series diode array and/or multiple wavelength detectors and Agilent 1100 Series fraction collector, controlled using ChemStation Rev.B02.01 and Purify version A.1.2 software.

Algal material. *Symphyocladia latiuscula* was collected on the coast of Qingdao, Shandong Province, China, in May 2004. The specimen identification was verified by Dr. Kui-Shuang Shao (Institute of Oceanology, Chinese Academy of Sciences, Qingdao 266071, China). A voucher specimen (No. 2004X16) was deposited at the Herbarium of the Institute of Oceanology, Chinese Academy of Sciences, Qingdao 266071, China.

Extraction and isolation. The air-dried red alga *Symphyocladia latiuscula* (4.3 kg) was extracted with 95% EtOH at room temperature (3 × 72 h). After the solvent was removed under reduced pressure at <40 °C, a dark residue (610 g) was obtained. The residue was partitioned between EtOAc and H_2O, and the EtOAc-soluble partition (320 g) was chromatographed over silica gel, eluting with a gradient of 0–100% Me_2CO/petroleum ether to yield 85 fractions (F1–F85) (see Supporting Information Scheme S1 for the fractionation scheme). Fraction F54 was further fractionated over Sephadex LH-20 using $CHCl_3$–MeOH (2:1) to afford 21 fractions.

The sixth fraction from Sephadex LH-20 chromatography was fractionated on an ODS column, eluted by a stepwise gradient (0–100% MeOH/H_2O) to afford 11 fractions. The third fraction was subjected to HPLC separation (Zorbax Eclipse XDB-C_8, 5 µm, 250 × 9.4 mm column, 3.0 mL/min, gradient elution from 10 to 80% $MeCN/H_2O$ over 15 min, with isocratic 0.01% TFA modifier) to yield **1–6**; the sixth fraction was subjected to HPLC separation (Zorbax SB-C_{18}, 5 µm, 250 × 9.4 mm column, 3.0 mL/min, gradient elution from 30 to 75% $MeCN/H_2O$ over 14 min, with isocratic 0.01% TFA modifier) to yield **8a/b** and **9a/b**; and the seventh fraction was subjected to HPLC separation (Zorbax Eclipse XDB-C_8, 5 µm, 250 × 9.4 mm column, 3.0 mL/min, gradient elution from 40 to 55% $MeCN/H_2O$ over 20 min, with isocratic 0.01% TFA modifier) to yield **11** and **13**.

The seventh fraction from Sephadex LH-20 chromatography was subjected to HPLC fractionation (Zorbax SB-C_{18}, 5 um, 250 × 9.4 mm column, 3.0 mL/min, gradient elution from 30 to 80% $MeCN/H_2O$ over 14 min, with isocratic 0.01% TFA modifier) to yield **10**.

The eighth fraction from Sephadex LH-20 chromatography was fractionated on an ODS column, eluted with a stepwise gradient (0–100% $MeOH/H_2O$) to afford 11 fractions; the sixth fraction was subjected to HPLC fractionation (Zorbax SB-C_{18}, 5 δm, 250 × 9.4 mm column, 3.0 mL/min, gradient elution from 35 to 50% $MeCN/H_2O$ over 15 min, with isocratic 0.01% TFA modifier) to yield **14**; the seventh fraction was subjected to HPLC fractionation (Zorbax SB-C_{18}, 5 µm, 250 × 9.4 mm column, 3.0 mL/min, gradient elution from 50 to 60% $MeCN/H_2O$ over 12 min, with isocratic 0.01% TFA modifier) to yield **12** and **15**.

The ninth fraction from Sephadex LH-20 chromatography was fractionated on an ODS column, eluted with a stepwise gradient (0–100% $MeOH/H_2O$) to afford 11 fractions; the third fraction was subjected to HPLC fractionation (Zorbax SB-C_{18}, 5 µm, 250 × 9.4 mm column, 3.0 mL/min, gradient elution from 30 to 80% $MeCN/H_2O$ over 20 min, with isocratic 0.01% TFA modifier) to yield **7a/b**.

Aconitate A (**1**): White solid; NMR (600 MHz, methanol-d_4) see Table S2; HRESIMS *m/z* 189.0396 $[M + H]^+$ (calcd. for $C_7H_8O_6$ 189.0394).

Aconitate B (**2**): White solid; NMR (600 MHz, methanol-d_4) see Table S2; HRESIMS *m/z* 189.0395 $[M + H]^+$ (calcd. for $C_7H_8O_6$ 189.0394).

Aconitate C (**3**): White solid; NMR (600 MHz, methanol-d_4) see Table S3; HRESIMS *m/z* 189.0395 $[M + H]^+$ (calcd. for $C_7H_8O_6$ 189.0394).

Aconitate D (**4**): White solid; NMR (600 MHz, methanol-d_4) see Table S3; HRESIMS *m/z* 203.0552 $[M + H]^+$ (calcd. for $C_8H_{11}O_6$, 203.0550)

Aconitate E (**5**): White solid; NMR (600 MHz, methanol-d_4) see Table S4; HRESIMS *m/z* 203.0551 $[M + H]^+$ (calcd. for $C_8H_{11}O_6$, 203.0550).

Aconitate F (**6**): White solid; NMR (600 MHz, methanol-d_4) see Table S4; HRESIMS *m/z* 217.0708 $[M + H]^+$ (calcd. for $C_9H_{13}O_6$, 217.0707).

Symphyocladins C/D (**7a/b**): Light brown solid; NMR (600 MHz, acetone-d_6) see Table 1, Table 2 and Table S5; HRESIMS *m/z* 544.8082 $[M + H]^+$ (calcd. for $C_{14}H_{12}Br_3O_8$, 544.8077).

Symphyocladins H/I (**8a/b**): Light brown solid; NMR (600 MHz, methanol-d_4, acetonitrile-d_3) see Table 1, Table 2, Tables S6 and S7; HRESIMS *m/z* 544.8081 $[M + H]^+$ (calcd. for $C_{14}H_{12}Br_3O_8$, 544.8077).

Symphyocladins J/K (**9a/b**): Light brown solid; NMR (600 MHz, DMSO-d_6) see Table 1, Table 2 and Table S8; HRESIMS *m/z* 558.8237 $[M + H]^+$ (calcd. for $C_{15}H_{14}Br_3O_8$, 558.8233).

Symphyocladin L (**10**): Light brown solid; NMR (600 MHz, acetone-d_6) see Table 3, Table 5 and Table S9; HRESIMS *m/z* 558.8238 $[M + H]^+$ (calcd. for $C_{15}H_{14}Br_3O_8$, 558.8233).

Symphyocladin M (**11**): Light brown solid; NMR (600 MHz, methanol-d_4) see Table 3, Table 5 and Table S10; HRESIMS *m/z* 586.8552 $[M + H]^+$ (calcd. for $C_{17}H_{17}Br_3O_8$, 586.8546).

Symphyocladin N (**12**): Light brown solid; NMR (600 MHz, acetone-d_6) see Table 4, Table 5 and Table S11; HRESIMS *m/z* 500.8184 $[M + H]^+$ (calcd. for $C_{13}H_{12}Br_3O_6$, 500.8179).

Symphyocladin O (**13**): Light brown solid; NMR (600 MHz, methanol-d_4) see Table 4, Table 5 and Table S12; HRESIMS *m/z* 530.8289 $[M + H]^+$ (calcd. for $C_{14}H_{14}Br_3O_7$, 530.8284).

Symphyocladin P (**14**): Light brown solid; NMR (600 MHz, methanol-d_4) see Table 4, Table 5 and Table S13; HRESIMS *m/z* 500.8184 $[M + H]^+$ (calcd. for $C_{13}H_{12}Br_3O_6$, 500.8179).

Symphyocladin Q (**15**): Light brown solid; NMR (600 MHz, acetone-d_6) see Table 3, Table 4 and Table S14; HRESIMS *m/z* 514.8340 $[M + H]^+$ (calcd. for $C_{14}H_{14}Br_3O_6$, 514.8335).

X-ray crystallography. X-ray crystallographic data were collected on an Oxford Diffraction Gemini CCD diffractometer with Mo-Kα radiation (0.71073 Å) operating within the range $2 < 2\theta < 50°$. The sample was cooled to 190 K with an Oxford Cryosystems Desktop Cooler. Data reduction and empirical absorption corrections were performed using CrysAlisPro (Rigaku Oxford Diffraction, Yarnton, Oxfordshire, UK). The structure was solved by Direct Methods and refined with SHELX [21] and all of the calculations and refinements were carried out by WinGX package [22]. All non-H atoms were refined aniostropically. The thermal ellipsoid plot was produced with ORTEP [23] and the unit cell diagram was drawn with PLATON [24]. Crystallographic data including structure factors in CIF format have been deposited with the Cambridge Crystallographic Data Centre (CCDC 1569026).

Supplementary Materials: The following are available online at www.mdpi.com/1660-3397/15/12/374/s1, Isolation Scheme as well as Tabulated 1D and 2D NMR data and spectra for 1–15, X-ray of compound **10**.

Acknowledgments: This work was supported in part by the Chinese Government Fundamental Research Funds for the Central Universities, the National Key Research and Development Program of China (2017YFD0201203), and the University of Queensland, Institute for Molecular Bioscience.

Author Contributions: X. Xu red alga collection, extractions, compound isolation and spectroscopic data analysis, H.Y. and L.Y. assisted in chemical fractionation, X. Xiao in acquisition of spectroscopic data. P.V.B. carried out X-ray analyses, and P.N. synthetic studies. F.S. acquired and analyzed spectroscopic data. Z.G.K., A.A.S. and R.J.C. analysed spectroscopic data and assembly the Supporting Information. R.J.C. proposed the biosynthesis. R.J.C. and F.S. managed the research, assigned structures, and co-drafted the manuscript.

Conflicts of Interest: The authors declare no conflict of interest.

References

1. Newman, D.J.; Cragg, G.M. Natural products as sources of new drugs from 1981 to 2014. *J. Nat. Prod.* **2016**, *79*, 629–661. [CrossRef] [PubMed]
2. Liu, M.; Hansen, P.E.; Lin, X.K. Bromophenols in marine algae and their bioactivities. *Mar. Drugs* **2011**, *9*, 1273–1292. [CrossRef] [PubMed]
3. Liu, X.; Li, X.M.; Gao, L.X.; Cui, C.M.; Li, C.S.; Li, J.; Wang, B.G. Extraction and PTP1B inhibitory activity of bromophenols from the marine red alga *Symphyocladia latiuscula*. *Chin. J. Oceanol. Limn.* **2011**, *29*, 686–690. [CrossRef]
4. Li, K.; Li, X.M.; Gloer, J.B.; Wang, B.G. New nitrogen-containing bromophenols from the marine red alga *Rhodomela confervoides* and their radical scavenging activity. *Food Chem.* **2012**, *135*, 868–872. [CrossRef] [PubMed]
5. Lin, X.K.; Liu, M. Bromophenols from marine algae with potential anti-diabetic activities. *J. Ocean Univ. China* **2012**, *11*, 533–538. [CrossRef]
6. Olsen, E.K.; Hansen, E.; Isaksson, J.; Andersen, J.H. Antioxidant effect of four bromophenols from the red algae *Vertebrata lanosa*. *Planta Med.* **2012**, *78*, 1146. [CrossRef]
7. Javan, A.J.; Javan, M.J.; Tehrani, Z.A. Theoretical investigation on antioxidant activity of bromophenols from the marine red alga *Rhodomela confervoides*: H-atom vs. electron transfer mechanism. *J. Agric. Food Chem.* **2013**, *61*, 1534–1541. [CrossRef] [PubMed]
8. Olsen, E.K.; Hansen, E.; Isaksson, J.; Andersen, J.H. Cellular antioxidant effect of four bromophenols from the red algae, *Vertebrata lanosa*. *Mar. Drugs* **2013**, *11*, 2769–2784. [CrossRef] [PubMed]
9. Xu, X.; Yin, L.; Gao, L.; Gao, J.; Chen, J.; Li, J.; Song, F. Two new bromophenols with radical scavenging activity from marine red alga *Symphyocladia latiuscula*. *Mar. Drugs* **2013**, *11*, 842–847. [CrossRef] [PubMed]
10. Xu, X.; Yin, L.; Gao, J.; Gao, L.; Song, F. Antifungal bromophenols from marine red alga *Symphyocladia latiuscula*. *Chem. Biodivers.* **2014**, *11*, 807–811. [CrossRef] [PubMed]
11. Kurata, K.; Amiya, T. Bis(2,3,6-tribromo-4,5-dihydroxybenzyl) ether from the red alga, *Symphyocladia latiuscula*. *Phytochemistry* **1980**, *19*, 141–142. [CrossRef]
12. Xu, X.; Song, F.; Fan, X.; Fang, N.; Shi, J. A novel bromophenol from marine red alga *Symphyocladia latiuscula*. *Chem. Nat. Compd.* **2009**, *45*, 811–813. [CrossRef]
13. Xu, X.; Piggott, A.M.; Yin, L.; Capon, R.J.; Song, F. Symphyocladins A–G: Bromophenol adducts from a Chinese marine red alga, *Symphyocladia latiuscula*. *Tetrahedron Lett.* **2012**, *53*, 2103–2106. [CrossRef]

14. Xu, X.; Yin, L.; Wang, Y.; Wang, S.; Song, F. A new bromobenzyl methyl sulphoxide from marine red alga *Symphyocladia latiuscula*. *Nat. Prod. Res.* **2013**, *27*, 723–726. [CrossRef] [PubMed]
15. Park, H.J.; Kurokawa, M.; Shiraki, K.; Nakamura, N.; Choi, J.S.; Hattori, M. Antiviral activity of the marine alga *Symphyocladia latiuscula* against herpes simplex virus (HSV-1) in vitro and its therapeutic efficacy against HSV-1 infection in mice. *Biol. Pharm. Bull.* **2005**, *28*, 2258–2262. [CrossRef] [PubMed]
16. Lee, J.H.; Park, S.E.; Hossain, M.A.; Kim, M.Y.; Kim, M.N.; Chung, H.Y.; Choi, J.S.; Yoo, Y.H.; Kim, N.D. 2,3,6-Tribromo-4,5-dihydroxybenzyl methyl ether induces growth inhibition and apoptosis in MCF-7 human breast cancer cells. *Arch. Pharm. Res.* **2007**, *30*, 1132–1137. [CrossRef] [PubMed]
17. Choi, J.S.; Park, H.J.; Jung, H.A.; Chung, H.Y.; Jung, J.H.; Choi, W.C. A cyclohexanonyl bromophenol from the red alga *Symphyocladia latiuscula*. *J. Nat. Prod.* **2000**, *63*, 1705–1706. [CrossRef] [PubMed]
18. Duan, X.J.; Li, X.M.; Wang, B.G. Highly brominated mono-and bis-phenols from the marine red alga *Symphyocladia latiuscula* with radical-scavenging activity. *J. Nat. Prod.* **2007**, *70*, 1210–1213. [CrossRef] [PubMed]
19. Wang, W.; Okada, Y.; Shi, H.B.; Wang, Y.Q.; Okuyama, T. Structures and aldose reductase inhibitory effects of bromophenols from the red alga *Symphyocladia latiuscula*. *J. Nat. Prod.* **2005**, *68*, 620–622. [CrossRef] [PubMed]
20. Jin, H.J.; Oh, M.Y.; Jin, D.H.; Hong, Y.K. Identification of a Taq DNA polymerase inhibitor from the red seaweed *Symphyocladia latiuscula*. *J. Environ. Biol.* **2008**, *29*, 475–478. [PubMed]
21. Sheldrick, G.M. A short history of SHELX. *Acta Crystallogr.* **2008**, *A64*, 112–122. [CrossRef] [PubMed]
22. Farrugia, L.J. ORTEP-3 for Windows-a version of ORTEP-III with a Graphical User Interface (GUI). *J. Appl. Crystallogr.* **1997**, *30*, 565. [CrossRef]
23. Farrugia, L.J. *WinGX* suite for small-molecule single-crystal crystallography. *J. Appl. Crystallogr.* **1999**, *32*, 837–838. [CrossRef]
24. Spek, A.L. PLATON, An integrated tool for the analysis of the results of a single crystal structure determination. *Acta Crystallogr. Sect A* **1990**, *46*, C34.